P-ISSN 2586-9000
E-ISSN 2586-9027
Homepage : https://tci-thaijo.org/index.php/SciTechAsia
Science & Technology Asia
Vol. 23 No.1 January - March 2018
Page: [ 30 - 38 ]
*Original research article*

# Manifold Ambiguities in Higher-Order Statistics-based Direction-Finding Systems

Supawat Supakwong[1,*]
[1]*Faculty of Engineering, Department of Electrical and Computer Engineering, Thammasat University, Pathumthani 12120, Thailand*

Received 22 November 2017; Received in revised form 12 December 2017
Accepted 15 January 2018; Available online 31 March 2018

**ABSTRACT**

Subspace-based direction-finding methods assume that all source's manifold vectors are linearly independent. However, when this condition is not satisfied, the estimation methods will subsequently fail to identify the directions of the sources. This undesirable effect is referred to as a manifold ambiguity. In this paper, the presence of manifold ambiguity associated to a higher-order statistics-based array processing is investigated. By analyzing the geometrical shape of the corresponding array manifold, a class of ambiguous sets based on a uniform partition of the effective manifold curve can be found. A general procedure is provided in order to model and categorize these ambiguities into the form of ambiguous generator sets.

**Keywords:** Manifold ambiguity; Direction-finding; Array processing; Higher-order of statistics

## 1. Introduction

The use of antenna array with smart signal processing algorithms to process and extract parameters of interest from the data has found a wide range of applications in recent years. Driven by the exploit of spatial domain, where multiple antennas work cooperatively as a single unit, this has emerged as a key technology for advancements in radars, sonars, wireless communications, as well as in speech and image enhancements [1-3].

Conventionally, array processing framework assumed signals are Gaussian, and processed using the second-order statistics. However, this assumption is not satisfied in some applications including digital communications where signals are non-Gaussian. To overcome with this limitation, research in [4-6] has shown that the array should process with the information embedded in a higher-orders of statistics (HOS). In [6], the Authors explored several advantages from using the fourth-order of statistics and proposed two algorithms for estimating the source' s directions-of-arrival (DOAs). This framework was then generalized in [7] with

***Corresponding author:** supawat@engr.tu.ac.th **doi:** 10.14456/scitechasia.2018.5

$2q-$order of statistics, where $q>1$. Interestingly, we can draw the relationships between the conventional second-order and the $2q-$order array processing via the virtual array concept [8,9]. This allows physical interpretation of the HOS-based processing, and indicates how it can significantly improve the array estimation performance [10].

Despite the ability to process with non-Gaussian signals, one issue that has not been addressed and needs to be carefully investigated is the presence of manifold ambiguities associated to HOS-based direction-finding systems. Manifold ambiguity represents an undesirable scenario when subspace-based direction-finding techniques, such as MUltiple SIgnal Classification(MUSIC) [11], and Estimation of Signal Parameters via Rotational Invariance Techniques(ESPRIT) [12], fail to uniquely identify the sources directions due to the linear dependence amongst array manifold vectors. This results in spurious peaks that do not represent the directions of the true sources. A number of factors contribute to the presence of manifold ambiguity. This include an array configuration, array size, the number of antennas, as well as inter-spacings between antennas [13-15].

There are infinitely many manifold ambiguities in practice. The result comes directly from the arc length rotational theorem [13]. Suppose an array suffers from an ambiguous situation when signals are simultaneously transmitted from a certain set of directions, measured in arc length, then any increment of this ambiguous set by $\triangle s$, also give another ambiguous scenario. Since $\triangle s$ can be arbitrary, this implies that once the ambiguity occurs, this can potentially create many more ambiguities by the same underlying cause.

Fig. 1 illustrates an example of the manifold ambiguity. On the solid red graph, the MUSIC algorithm indicates 3 peaks at the directions $8.81^{\circ}, 85.46^{\circ}, 146.10^{\circ}$. While the peaks at $8.81^{\circ}$, and $146.10^{\circ}$ correctly identify the source's directions, another peak from $85.46^{\circ}$ is spurious and does not represent the true source. Its presence is mainly due to the linear dependence amongst the array manifold vectors from these three directions. Meanwhile, the spectrum in dashed blue represents another ambiguous scenario caused by the same factor, with $\triangle s = 1.5$.

Different approaches have been proposed to minimize or suppress the presence of manifold ambiguities. The key is to breakdown the linear dependence amongst manifold vectors. For instance, in [16,17], the Authors analyzed the conditions on array configurations such that manifold ambiguities of a certain rank can be avoided. In [18-21], different methods are proposed to identify a correct set of DOAs, either by using the estimated signal power as an indicator [18,19], or substrate placement [20,21].

It should be noted that all above-mentioned work are focused entirely on the ambiguities with respect to the second-order statistics. Ambiguities associated to HOS-based direction-finding has not been investigated anywhere before, and essentially be our objective herein.

The organization for the remaining of the paper is as follows. In the next Section, a signal modelling based on $2q-$order is presented, together with the virtual array concept. In Section 3, the geometrical properties of HOS-based array manifold are assessed using differential geometry framework. A general guideline to determine an ambiguous generator set (AGS) is subsequently provided. Computer simulation is presented in Section 4, followed by a conclusion in section 5.

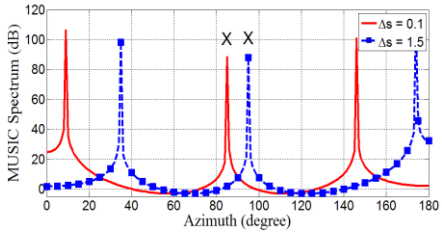


**Fig. 1.** An example of manifold ambiguities with respect to the array listed in Eq. (4.1).

## 2. Problem Formulation

### 2.1 Signal Modelling

Consider a linear array of $N$ antennas located at the position $\underline{r}_x$ measured in half wavelength, operated in the presence of $M$ narrow-band point sources impinging from the array far-field with azimuth directions $\theta_i, i \in \{1,\ldots,M\}$. The baseband received signal vector $\underline{x}(t) \in C^{N\times 1}$ from each antenna represents a superposition of $M$ incoming waveforms, expressed as

$$\begin{aligned}\underline{x}(t) &= \left[x_1(t), x_2(t), \ldots, x_N(t)\right]^T, \\ &= \sum_{i=1}^{M} \underline{\mathbf{a}}(\theta_i) m_i(t) + \underline{n}(t),\end{aligned} \tag{2.1}$$

where $m_i(t)$ is the $i^{th}$ message signal, $\underline{n}(t)$ is zero-mean white Gaussian noise with the variance $\sigma^2$ and the vector $\underline{\mathbf{a}}(\theta_i)$ denotes an array manifold vector for the $i^{th}$ incoming source, expressed as

$$\underline{\mathbf{a}}(\theta_i) = \exp\left(-j\pi \underline{r}_x \cos\theta_i\right) \tag{2.2}$$

Conventional array processing techniques exploit the information contained in the second-order covariance matrix $\mathbb{R}_{xx} \in C^{N\times N}$, where

$$\begin{aligned}\mathbb{R}_{xx} &= E\left\{\underline{x}(t)\underline{x}^H(t)\right\} \\ &= \sum_{i=1}^{M} c_{2,m_i} \underline{\mathbf{a}}(\theta_i)\underline{\mathbf{a}}^H(\theta_i) + \sigma^2 \mathbb{I}_N\end{aligned} \tag{2.3}$$

with $c_{2,m_i}$ denotes the message signal power, $(\,)^H$ is the Hadamard operation (conjugate-transpose) and $\mathbb{I}_N$ is an $(N \times N)$ identity matrix.

### 2.2 Higher-Order of Statistics and the Virtual Antenna Array

To process non-Gaussian signals, HOS-based array processing exploits the information contained in a covariance matrix of a higher-order. Denoting the order by using $2q$, where $q > 1$, the array extracts the information from the $\left(N^q \times N^q\right)$ circular covariance matrix $\mathbb{C}_{2q,x}$ of

$$\begin{aligned}\mathbb{C}_{2q,x}(l) = \sum_{i=1}^{M} c_{2q,m_i} &\left[\underline{\mathbf{a}}(\theta_i)^{\otimes l} \otimes \underline{\mathbf{a}}(\theta_i)^{*\otimes(q-l)}\right] \\ &\times \left[\underline{\mathbf{a}}(\theta_i)^{\otimes l} \otimes \underline{\mathbf{a}}(\theta_i)^{*\otimes(q-l)}\right]^H,\end{aligned} \tag{2.4}$$

where the vector $\underline{\mathbf{a}}(\theta_i)^{\otimes l}$ denotes the Kronecker products over $l$ terms of $\underline{\mathbf{a}}(\theta_i)$, i,e,

$$\underline{\mathbf{a}}(\theta_i)^{\otimes l} = \underbrace{\underline{\mathbf{a}}(\theta_i) \otimes \underline{\mathbf{a}}(\theta_i) \otimes \ldots \otimes \underline{\mathbf{a}}(\theta_i)}_{l \text{ terms}}. \tag{2.5}$$

The integer $0 \le l \le q$ relates to the arrangement of $\mathbb{C}_{2q,x}(l)$. The study in [8] showed that the processing power is maximized when $l = \left\lceil \frac{q}{2} \right\rceil$.

By comparing $\mathbb{C}_{2q,x}$ in Eq. (2.4) to $\mathbb{R}_{xx}$ in Eq. (2.3), we can draw some relationships between the second order and a HOS referred to as the virtual array concept [8]. Specifically, the terms $\underline{\mathbf{a}}(\theta_i)^{\otimes l} \otimes \underline{\mathbf{a}}(\theta_i)^{*\otimes(q-l)}$ in Eq. (2.4) can be compared to the vector $\underline{\mathbf{a}}(\theta_i)$ in Eq. (2.3),

and viewed as being an effective second-order manifold vector $\underline{\mathbf{a}}_e(\theta_i)$, where

$$\underline{\mathbf{a}}_e(\theta_i) = \underline{\mathbf{a}}(\theta_i)^{\otimes l} \otimes \underline{\mathbf{a}}(\theta_i)^{*\otimes(q-l)} \qquad (2.6)$$

Follow through the derivation in [8], the effective manifold vector $\underline{\mathbf{a}}_e(\theta_i)$ can be expressed as

$$\underline{\mathbf{a}}_e(\theta_i) = \exp\left\{-j\pi \underline{r}_{x,e}^T \cos\theta_i\right\}, \qquad (2.7)$$

where $\underline{r}_{x,e}$ represents the position of the virtual array, in the form

$$\underline{r}_{x,e}^T = \left(\underline{r}_x^T\right)^{\oplus l} \ominus \left(\underline{r}_x^T\right)^{\oplus(q-l)}. \qquad (2.8)$$

The operators $\oplus$ and $\ominus$ denote the Kronecker addition and subtraction accordingly.

In another word, the HOS-based array processing with the matrix $\mathbb{C}_{2q,x}$ can be viewed as being equivalent to the conventional array processing with the antenna array virtually located at $\underline{r}_{x,e}$.

To illustrate this concept, let us consider an example of a linear array of 3 antennas, located at $\underline{r}_x = [-1,0,1]^T$ measured in half wavelength. If the array is processed using the fourth-order of statistics $(q=2)$ with $l = \left\lceil \frac{q}{2} \right\rceil = 1$, this is equivalent to the second-order array processing with the virtual array located at

$$\underline{r}_{x,e}^T = \underline{r}_x^T \ominus \underline{r}_x^T = [-2,-1,0,1,2]^T.$$

This virtual array consists of 5 antennas and the aperture of 4.

Suppose, now, the array is processed using the $6^{th}-$order statistics $(q=3)$ and $l = \left\lceil \frac{q}{2} \right\rceil = 2$. The virtual array is in the form,

$$\begin{aligned}\underline{r}_{x,e}^T &= \left(\underline{r}_x^T\right)^{\oplus 2} \ominus \underline{r}_x^T = \left(\underline{r}_x^T \oplus \underline{r}_x^T\right) \ominus \underline{r}_x^T \\ &= [-3,-2,-1,0,1,2,3]^T,\end{aligned}$$

where it consists of 7 virtual antennas and the aperture of 6 half wavelength. Similarly, the $8^{th}-$order array processing with $q=4$ and $l = \left\lceil \frac{q}{2} \right\rceil = 2$, is equivalent to the conventional second-order array processing with

$$\begin{aligned}\underline{r}_{x,e}^T &= \left(\underline{r}_x^T\right)^{\oplus 2} \ominus \left(\underline{r}_x^T\right)^{\oplus 2} \\ &= \left(\underline{r}_x^T \oplus \underline{r}_x^T\right) \ominus \left(\underline{r}_x^T \oplus \underline{r}_x^T\right) \\ &= [-4,-3,-2,-1,0,1,2,3,4]^T.\end{aligned}$$

It is clearly seen that by using a HOS, the array is effectively enlarged, both in terms of the size and the number of virtual antennas, as summarized in Table 1. That explains why the array can process with more sources, and the performance is improved when using a HOS.

**Table 1.** Virtual antenna array with respect to $2q-$orders of statistics

| Order | Configuration | Aperture | $N_{vs}$ |
|---|---|---|---|
| 2 | $[-1,0,1]^T$ | 2 | 3 |
| 4 | $[-2,-1,0,1,2]^T$ | 4 | 5 |
| 6 | $[-3,-2,-1,0,1,2,3]^T$ | 6 | 7 |
| 8 | $[-4,-3,-2,-1,0,1,2,3,4]^T$ | 8 | 9 |

## 3. Manifold Ambiguities in HOS-based Array Systems

By definition, manifold ambiguity represents the array inability to identify a correct set of DOAs due to linear dependence amongst signal manifold vectors [14]. Several factors contribute to this undesirable situation including the array size, number of antennas, as well as array

configuration especially in terms of the antenna's inter-spacing.

### 3.1 Ambiguous Generator Set (AGS)

The studies in [13,14] investigated the causes of manifold ambiguity by analyzing array manifold from the differential geometry perspective. Defined as a locus of all manifold vectors over the field of view, the manifold can be visualized as being a geometrical object embedded in a high-dimensional complex space. For instance, the locus of all manifold vectors $\underline{\mathbf{a}}(\theta_i)$, for $\theta_i \in [0^\circ, 180^\circ)$ represents a curve embedded in an $N-$dimensional complex space, i.e.

$$\mathcal{A} = \left\{ \underline{\mathbf{a}}(\theta) \in \mathcal{C}^{N\times 1}, \forall \theta : \theta \in [0^\circ, 180^\circ) \right\}. \tag{3.1}$$

Differential geometry is a tool used to assess the shape of this array manifold. For instance, the curve can be characterized in the form of arc length $s$,

$$s(\theta) = \int_0^\theta \left\| \frac{d\underline{\mathbf{a}}}{d\theta} \right\| d\theta \tag{3.2}$$

The detailed analysis in [14] showed that the presence of manifold ambiguity is fundamentally related to the geometrical properties of the manifold. That is, suppose we take the total length $l_m$ of the manifold curve, where $l_m = 2\pi \|\underline{r}_x\|$, and uniformly partition the curve into equal segments of

$$\begin{aligned} \underline{s}_{\triangle r_{ij}} &= [s_0, s_1, \ldots, s_c]^T, \\ &= \left[ 0, \frac{l_m}{\triangle r_{ij}}, \frac{2l_m}{\triangle r_{ij}}, \ldots, \frac{(c-1)l_m}{\triangle r_{ij}} \right]^T, \end{aligned} \tag{3.3}$$

where $\triangle r_{ij} \triangleq |r_i - r_j|$ denotes the inter-spacing between the $i^{th}$ and $j^{th}$ antennas, and $c > N$. If the matrix $\mathbb{A}(\underline{s}_{\triangle r_{ij}})$ that corresponds to the manifold matrix of this set of arc length,

$$\mathbb{A}(\underline{s}_{\triangle r_{ij}}) = [\underline{\mathbf{a}}(s_0), \underline{\mathbf{a}}(s_1), \ldots, \underline{\mathbf{a}}(s_c)], \tag{3.4}$$

is rank-deficient, then any subset of $\underline{s}_{\triangle r_{ij}}$ with $N$ elements represents an ambiguous set of directions.

In addition, the arc length rational theorem from [14] showed that for any increment of $\underline{s}_{\triangle r_{ij}}$ by $\triangle s$, i,e,

$$\underline{s}_{\triangle r_{ij}} + \triangle s = \left[ \triangle s, \frac{l_m}{\triangle r_{ij}} + \triangle s, \ldots, \frac{(c-1)l_m}{\triangle r_{ij}} + \triangle s \right]^T \tag{3.5}$$

where $\frac{(c-1)l_m}{\triangle r_{ij}} + \triangle s < l_m$, the matrix $\mathbb{A}(\underline{s}_{\triangle r_{ij}} + \triangle s)$ is also rank-deficient. Consequently, with $\triangle s$ being arbitrary, there are infinitely many ambiguous sets of directions. For this reason, it is better to categorize these ambiguous sets of directions in the form of Ambiguous Generator Set (AGS) [14].

### 3.2 HOS-based Manifold Ambiguity

Our discussion so far has focused mainly on manifold ambiguity with respect to the conventional second-order direction-finding techniques. To proceed to the analysis of HOS-based manifold ambiguity, we need to characterize the geometrical properties of the HOS-based array manifold, which is defined as

$$\mathcal{A}_e = \left\{ \underline{\mathbf{a}}_e(\theta) \in \mathcal{C}^{N_{vs}\times 1}, \forall \theta : \theta \in [0^\circ, 180^\circ) \right\}, \tag{3.6}$$

where $N_{vs}$ represents the total number of virtual antennas. The detailed analysis of these array manifold for different orders of statistics can be found in [10]. Essentially, with a HOS, the manifold curve is longer in length with

$$l_{m,e} = 2\pi \|\underline{r}_{x,e}\|. \tag{3.7}$$

Meanwhile, regardless of the order, the principle curvature $\kappa_{i,e}(s)$ of the curve remains constant at any point. That implies the curves have the hyperhelical shape. This is an important finding because the proposed procedure to identify HOS-based ambiguity requires the corresponding manifold curve with a hyperhelical shape.

From this finding, together with the virtual antenna concept, a class of $2q-$order manifold ambiguity may be found. A general procedure to determine the presence of ambiguity generator set in a HOS is provided as follows.

1. For a given $2q-$order, form the virtual array using Eq.(2.8) Calculate the number of virtual antennas $N_{vs}$ and the corresponding array aperture.

2. Compute inter-spacings between antennas $\forall i, j \in \{1,\ldots,N_{vs}\}$,

$$\triangle r_{ij,e} \triangleq \left| r_{i,e} - r_{j,e} \right| \qquad (3.8)$$

3. Form the $2q-$manifold curve. Compute the effective manifold curve length $l_{m,e}$ using Eq. (3.7).

4. Form the uniform basic sets(UBS) $\underline{s}_{\triangle r_{ij,e}}$,

$$\underline{s}_{\triangle r_{ij,e}} = \left[ 0, \frac{l_{m,e}}{\triangle r_{ij,e}}, \ldots, \frac{(c-1)l_{m,e}}{\triangle r_{ij,e}} \right]^T . \qquad (3.9)$$

If the matrix $\mathbb{A}\left(\underline{s}_{\triangle r_{ij,e}}\right)$ is rank-deficient, then any $N_{vs}$ elements subset give an ambiguous set.

5. Evaluate the AGS according to the definition in [14].

## 4. Simulation Studies

In this Section, a modelling and identification of HOS-based manifold ambiguity in the form of AGS shall be presented.

Consider a linear array system consisting of $N=3$ antennas located at

$$\underline{r}_x = [-2, 0.2, 1.8]^T , \qquad (4.1)$$

measured in half-wavelength. Assume the array is operated in the presence of $M$ narrow-band point sources, where signals are zero-mean non-Gaussian.

Let's first analyze the presence of manifold ambiguity in the conventional second-order array processing. According to an array manifold curve $\mathcal{A}$, given by

$$\mathcal{A} = \left\{ \underline{\mathbf{a}}(\theta) \in \mathcal{C}^{N\times 1}, \forall \theta : \theta \in \left[ 0^{\circ}, 180^{\circ} \right) \right\}, \quad (4.2)$$

with the total length $l_m = 2\pi \left\| \underline{r}_x \right\| = 16.95$, the uniform basic sets are obtained from partitioning the manifold curve length $l_m$ by the inter spacing between antennas.

In this example, there are three unique inter-spacing namely, $\triangle r_{12} = 2.2$, $\triangle r_{13} = 3.8$, and $\triangle r_{23} = 1.6$. The corresponding UBSs are as follows,

$$\underline{s}_{\triangle r_{12}} = \left[ 0, 7.706, 15.412 \right]^T ,$$

$$\underline{s}_{\triangle r_{13}} = \left[ 0, 4.461, 8.923, 13.384 \right]^T ,$$

$$\underline{s}_{\triangle r_{23}} = \left[ 0, 10.596 \right]^T .$$

While the manifold matrix $\mathbb{A}\left(\underline{s}_{\triangle r_{23}}\right)$ corresponding to the set $\underline{s}_{\triangle r_{23}}$ is not rank-deficient, and does not satisfy the conditions of AGS, the UBS $\underline{s}_{\triangle r_{12}}$ represents an AGS of rank-2, and $\underline{s}_{\triangle r_{13}}$ gives rise to three AGSs of rank-2 as shown in Table 2.

Each one of these AGSs may be viewed as a generator for the infinitely many ambiguous sets of directions according to the arc length rotational theorem. For instance, Fig. 1 shows ambiguous situation that is caused by the first AGS, when $\triangle s_1 = 0.1$ and $\triangle s_2 = 1.5$ accordingly.

**Table 2.** Ambiguous generator sets according to the 2nd order of statistics

| | $\triangle r_{ij}$ | AGS | Rank |
|---|---|---|---|
| 1 | $\triangle r_{12}$ | [0, 7.706, 15.412] | 2 |
| 2 | $\triangle r_{13}$ | [0, 4.461, 8.923] | 2 |
| 3 | $\triangle r_{13}$ | [0, 4.461, 13.384] | 2 |
| 4 | $\triangle r_{13}$ | [0, 8.923, 13.384] | 2 |

Proceeding to the HOS-based array processing, the array is virtually increased both in terms of the sizes, and the number of virtual antennas, as seen in Table 3. This significantly improves the overall array performance.

**Table 3.** The virtual antenna array for different orders of statistics

| $2q$ | Array position $\underline{r}_{x,e}$ | aperture | $N_{vs}$ |
|---|---|---|---|
| 2 | $[-2, 0.2, 1.8]^T$ | 3.8 | 3 |
| 4 | $[-3.8, -2.2, -1.6, 0, 1.6, 2.2, 3.8]^T$ | 7.6 | 7 |
| 6 | [-5.8, -4.2, -3.6, -2.0, -1.4, -0.4, 0.2, 1.8, 2.4, 3.4, 4.0, 5.6]$^T$ | 11.4 | 12 |

From the differential geometry, the manifold curve corresponding to $2q-$order array processing, defined as

$$\mathcal{A}_e = \left\{ \underline{\mathbf{a}}_e(\theta) \in \mathcal{C}^{N_{vs}\times 1}, \forall \theta : \theta \in \left[0^\circ, 180^\circ\right) \right\}, \quad (20)$$

is varied according to the order $2q$. The curves are longer in general, while maintain a hyperhelical shape with a constant principle curvature $\kappa_i(s)$, as shown in Table 4.

**Table 4.** Geometrical properties of the effective manifold curves

| 2q | $s_e(\theta)$ | $l_{m,e}$ | $\kappa_i$ |
|---|---|---|---|
| 2 | $8.48(1-\cos\theta)$ | 16.95 | 0.71 |
| 4 | $20.76(1-\cos\theta)$ | 41.53 | 0.50 |
| 6 | $36.95(1-\cos\theta)$ | 73.90 | 0.40 |

Following the general procedure listed in Section 3, we can identify a class of AGS for different orders of statistics as follows:

***The 4th order AGS***

From the virtual antennas listed in Table 3, where

$$\underline{r}_{x,e} = \left[ r_1, r_2, \ldots, r_{N_{vs}} \right]^T = \left[-3.8, -2.2, -1.6, 0, 1.6, 2.2, 3.8\right]^T$$

that consists of 7 antennas. There are 9 unique inter-spacings as follows,

$$\begin{aligned}
&\triangle r_{12} = \triangle r_{34} = \triangle r_{67} = \triangle r_{45} = 1.6\\
&\triangle r_{13} = \triangle r_{24} = \triangle r_{46} = \triangle r_{57} = 2.2,\\
&\triangle r_{14} = \triangle r_{25} = \triangle r_{36} = \triangle r_{47} = 3.8,\\
&\triangle r_{15} = \triangle r_{37} = 5.4,\\
&\triangle r_{16} = \triangle r_{27} = 6,\\
&\triangle r_{17} = 7.6,\\
&\triangle r_{23} = \triangle r_{56} = 0.6,\\
&\triangle r_{26} = 4.4,\\
&\triangle r_{35} = 3.2.
\end{aligned}$$

With the total length of the 4th order manifold curve is equal to $l_m = 41.53$, 8 different uniform basic sets can be formed,

$$\begin{aligned}
&\underline{s}_{\triangle r_{12}} = [0, 25.95]^T,\\
&\underline{s}_{\triangle r_{13}} = [0, 18.88, 37.75]^T,\\
&\underline{s}_{\triangle r_{14}} = [0, 10.93, 21.86, 32.78]^T,\\
&\underline{s}_{\triangle r_{15}} = [0, 7.69, 15.38, 23.07, 30.76, 38.45]^T,\\
&\underline{s}_{\triangle r_{16}} = [0, 6.92, 13.84, 20.76, 27.68, 34.61]^T,\\
&\underline{s}_{\triangle r_{17}} = [0, 5.46, 10.93, 16.39, 21.86, 27.32, 32.78, 38.25]^T,\\
&\underline{s}_{\triangle r_{26}} = [0, 9.44, 18.88, 28.31, 37.75]^T,\\
&\underline{s}_{\triangle r_{35}} = [0, 12.98, 25.95, 38.93]^T.
\end{aligned}$$

Further evaluation shows that only four sets from $\underline{s}_{\triangle r_{14}}, \underline{s}_{\triangle r_{15}}, \underline{s}_{\triangle r_{16}}$, and $\underline{s}_{\triangle r_{17}}$ create rank-deficient manifold matrix. Consequently,

the ambiguous generator sets are obtained as shown in Table 5.

**Table 5.** Ambiguous generator sets according to the 4th order of statistics

| | $\Delta r_{ij}$ | AGS | Rank |
|---|---|---|---|
| 1 | $\Delta r_{14}$ | $[0, 10.93, 21.86, 32.78]^T$ | 3 |
| 2 | $\Delta r_{15}$ | $[0, 7.69, 15.38, 23.07, 30.76, 38.45]^T$ | 5 |
| 3 | $\Delta r_{16}$ | $[0, 6.92, 13.84, 20.76, 27.68, 34.61]^T$ | 5 |
| 4 | $\Delta r_{17}$ | $[0, 5.46, 16.39, 27.32, 38.25]^T$ | 4 |
| 5 | $\Delta r_{17}$ | $[0, 10.93, 21.86, 32.79]^T$ | 3 |

***The 6th order AGS***

Following the same procedure, we can obtain a class of ambiguous generator set associated with the 6th order of statistics. The effective antenna array is listed in Table 3, where it consists of 12 virtual antennas. There are total of 18 unique inter-spacings.

With the associated manifold curve length is equal to $l_m = 73.90$, 18 uniform basic sets were formed using Eq. (3.9). However, only one of these UBSs creates a rank-deficient manifold matrix, and consequently be an AGS, with the rank of ambiguity equals to 11,

$$\underline{s}_{\Delta r_{1,12}} = [0, 6.48, 12.96, 19.45, 25.93, 32.41, 38.89, 45.37, 51.86, 58.34, 64.82, 71.30]^T$$

From this example, one may note that different orders of statistics give rises to different sets of AGS. This implies that an ambiguous scenario with one order of statistic is not necessary to be ambiguous when processing with another order. For instance, shown in Fig. 2, all of the AGSs associated to the second-order of statistics in Table 2 disappear when the array is processed with either the 4th or 6th orders. This certainly provides another effective approach, in addition to [18-21], in resolving the presence of manifold ambiguities.

Another interesting point to observe is the associated rank of ambiguity corresponding to each order of statistics. In general, when the order $2q$ is increased, the rank of ambiguity is also increased. From this example, all of the second-order AGSs have rank-2 ambiguities, while the 4th order AGSs consist of rank 3, 4, and 5, and the 6th order AGS has rank-11 accordingly.

While the severity of manifold ambiguity does not relate to its rank, we can practically claim that a higher-rank ambiguity is more difficult to be encountered. For instance, if the presence of rank-2 ambiguity is compared to rank-11 ambiguity, the first ambiguous scenario occurs as soon as three sources from the specific directions laid out by the AGS are simultaneously transmitted. On the other hand, for rank-11 ambiguity to occur, that requires 12 simultaneously transmitted sources with very specific set of directions.

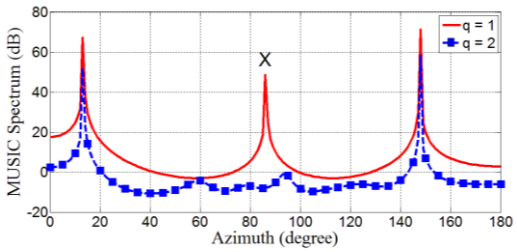


**Fig. 2.** Comparision of MUSIC spectrums when the array is processed using the 2nd (solid red) and 4th (dashed blue) orders of statistics.

## 5. Conclusions

The presence of manifold ambiguity associated to a HOS-based direction-finding systems was investigated in this paper. From differential geometry perspective, it was shown that ambiguity is fundamentally related to an array geometry, especially in terms of the antenna's inter-spacings. With the virtual array concept and the corresponding effective array manifold, a general procedure was presented to identify and categorize HOS-based manifold

ambiguity in the form of ambiguous generator sets.

## References


[1] Naidu PS. Sensor array signal processing. CRC Press; 2017.

[2] Van Trees HL. Optimum array processing: part IV of detection, estimation and modulation theory. Wiley; 2012.

[3] Haykin S, Liu KJR. Handbook on Array Processing and Sensor Networks. Wiley-IEEE Press; 2010.

[4] Dogan MC, Mendel JM. Applications of cumulants to array processing (i) aperture extension and array calibration. IEEE Transactions on Signal Processing 1995;43(5):1200–1216.

[5] Dogan MC, Mendel JM. Applications of cumulants to array processing. (ii) non-Gaussian noise suppression. IEEE Transactions on Signal Processing 1995; 43(7):1663–1676.

[6] Porat B, Friedlander B. Direction finding algorithms based on high-order statistics. IEEE Transactions on Signal Processing 1991;39(9):2016–2024.

[7] Chevalier P, Ferreol A, Albera L. High-resolution direction finding from higher order statistics: The $2q-$MUSIC algorithm. IEEE Transactions on Signal Processing 2006;54(8):2986–2997.

[8] Chevalier P, Ferreol A. On the virtual array concept for the fourth-order direction finding problem. IEEE Transactions on Signal Processing 1999;47(9):2592–2595.

[9] Chevalier P, Albera L, Ferreol A, Comon P. On the virtual array concept for higher order array processing. IEEE Transactions on Signal Processing 2005;53(4):1254–1271.

[10] Supakwong S. Performance Improvement of Subspace-Based Direction-Finding Algorithms Using Higher-Order Statistics. International Review of Electrical Engineering (IREE) 2015;10:42-51.

[11] Schmidt R. Multiple emitter location and signal parameter estimation. IEEE Trans. on Antennas and Propagation 1986; 34:276-280.

[12] Roy R, Kailath T. ESPRIT-estimation of signal parameters via rotational invariance techniques. IEEE Trans. on Acoustics, Speech, and Signal Processing 1989;37: 984-995.

[13] Manikas A, Proukakis C. Modeling and estimation of ambiguities in linear arrays. IEEE Trans. on Signal Processing 1998;46:2166–2179.

[14] Manikas A. Differential geometry in array processing. London: Imperial College Press; 2004.

[15] Manikas A, Proukakis C, Lefkaditis V. Investigative study of planar array ambiguities based on hyperhelical parameterization. IEEE Transactions on Signal Processing 1999;47: 1532-1541.

[16] Tan KC, Say SG, Tan EC. A study of the rank-ambiguity issues in direction-of-arrival estimation. IEEE Trans. on Signal Processing 1996;44: 880–887.

[17] Tan KC, Goh Z. A detailed derivation of arrays free of higher rank ambiguities. IEEE Trans. on Signal Processing 1996;44: 351-359.

[18] Supakwong S, Manikas A, Constantinides AG. Resolving manifold ambiguities in direction finding systems. EUSIPCO Proceedings 2007: 95-99.

[19] Abramovich YI, Spencer NK, Gorokhov AY. Resolving manifold ambiguities in direction-of-arrival estimation for nonuniform linear antenna arrays. IEEE Trans. on Signal Processing 1999;47: 2629-2643.

[20] He Z, Zhao Z, Nie Z, Ma P, Liu Q. Resolving manifold ambiguities for sparse array using planar substrates. IEEE Transactions on Antennas and Propagation 2012;60:2558 –2562.

[21] Supakwong S. The general procedure for resolving manifold ambiguity using planar substrate placement. IEEE Vehicular Technology Conference Proceeding 2013:1-